Int J Fract (2008) 150:221–226
DOI 10.1007/s10704-008-9219-1

ORIGINAL PAPER

Mechanics of hierarchical materials

Alberto Carpinteri · Nicola Maria Pugno

Received: 3 April 2008 / Accepted: 17 May 2008 / Published online: 8 July 2008

Abstract In this paper the simplest mathematical model to design nano-bio-inspired hierarchical materials is proposed. Simple formulas describing the dependence of strength, toughness and stiffness on the considered size-scale are derived, taking into account the toughening biomechanisms.

Keywords Strength · Fracture · Hierarchical · Nano · Bio · Materials

1 Introduction

Biological materials exhibit several levels of hierarchy, from the nano- to the macro-scale. For instance, sea shells have 2 or 3 orders of lamellar structures, as well as bone, similarly to dentin, has 7 orders of hierarchy (Currey 1977, 1984). These nano-bio-materials are composed by hard and strong mineral structures embedded in a soft and tough protein matrix. In bone and dentin, the mineral platelets are $\sim$3 nm thick, whereas in shells their thickness is of $\sim$300 nm, with very high slenderness. With this hard/soft nano-hierarchical texture, Nature seems to suggest us the key for optimizing materials with respect to both strength and toughness, without losing stiffness. Even if hierarchical materials are recognized to possess a fractal-like topology (Lakes 1993), only few engineering models explicitly considering their complex structure are present in the literature (see Gao 2006, Pugno 2006 and related references). In this letter, a concise mathematical model is presented, based on the force equilibrium. An energy formulation has been recently proposed by Pugno and Carpinteri (2008).

A. Carpinteri · N. M. Pugno (✉)
Department of Structural Engineering, Politecnico di Torino,
Corso Duca degli Abruzzi 24, 10129 Torino, Italy
e-mail: nicola.pugno@polito.it

2 The mathematical model

Strength, toughness and stiffness of materials are measured by tensile tests. Imagine a virtual tensile test on a hierarchically fibre-reinforced bar. Its cross-section, composed by hard inclusions embedded in a soft matrix, is schematized in Fig. 1.

The smallest units, at the level N, are considered scale-invariant and related to the theoretical material strengths of the hard and soft phases, respectively σ_h, σ_s, where usually $\sigma_h \gg \sigma_s$. Each inclusion at the level $k+1$ contains n_k smaller ones, each of them with cross-sectional area A_k. Thus, the total number of inclusions at the level k is

$$N_k = \prod_{j=1}^{k} n_j .$$

The *equilibrium equation* is $F \equiv A\sigma_C = F_h + F_s = N_k A_k \sigma_{hk} + (A - N_k A_k)\,\sigma_{sk} = N_N A_N \sigma_{hN} + (A - N_N A_N)\,\sigma_{sN}$, $\forall k$, where F is the critical applied force, F_h, F_s are the forces carried by the hard and soft phases respectively, $A \equiv A_0$ is the cross-section area of the bar, σ_C is its strength, $\sigma_{hN} \equiv \sigma_h$, $\sigma_{sk} \equiv \sigma_s$ ($\forall k$), and the subscript k refers to the quantities at the level k. Note that

$$\varphi_k = \frac{n_{k+1} A_{k+1}}{A_k}$$

represents the cross-sectional fraction of the inclusions at the level $k+1$ in the inclusions at the level k.

Natural optimization suggests self-similar structures (Brown and West 1999), for which $n_k = n$ and $\varphi_k = \varphi$, thus k-independent numbers and fractions; accordingly $N_k = n^k$. Since the inclusions present a fractal distribution (Carpinteri and Pugno 2005), we expect $F_h \propto R^D$ where $R = \sqrt{A}$ is a characteristic size and D is a constant, the so-called "fractal exponent"; the constant of proportionality can be deduced noting that $F_h\,(A = A_N) = A_N \sigma_{hN}$, and thus $F = \sigma_{hN} R_N^{2-D} R^D$. Accordingly, from $F_h = \sigma_{hN} R_N^{2-D} R^D = \sigma_{hN} n^N R_N^2$, we derive:

$$N = D \frac{\ln R/R_N}{\ln n}, \tag{1}$$

that defines the number of hierarchical levels that we need to design an object of characteristic size R. Equation 1 shows that only few hierarchical levels are required for spanning several orders of magnitude in size. For example, for a nano-structured hierarchical "universe", considering for R its actual radius, i.e., $R \approx 10^{26}$ m, for the smallest units a

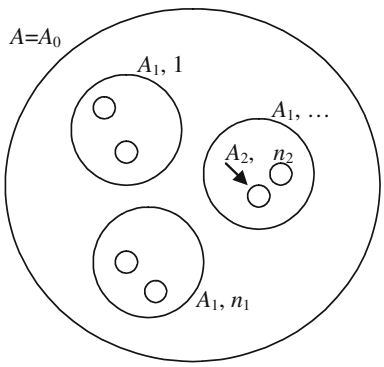

Fig. 1 The cross-section of a hierarchical bar

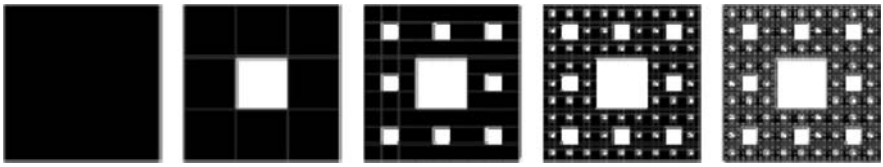

Fig. 2 The Sierpinski carpet ($D = 1.89$) at different level of observation; it corresponds to a deterministic hierarchical bar in which the empty space is the soft matrix, and the complementary zones are the hard inclusions

radius on 1 nm, i.e., $R_N \approx 10^{-9}$ m, $n = 5$ and $D = 2$ would result in only 100 hierarchical levels.

The scaling exponent D can be determined noting that $A - N_N A_N = A\,(1 - \phi)$, where $\phi = \varphi^N$ represents the macroscopic (at level 0) cross-sectional fraction of the hard inclusions. Thus, we derive $R/R_N = (n/\varphi)^{N/2}$. Introducing this result into Eq. 1 provides the fractal exponent, as a function of well-defined physical quantities:

$$D = \frac{2 \ln n}{\ln n - \ln \varphi}. \tag{2}$$

Note that D represents the fractal dimension of the inclusions, i.e., of a lacunar two-dimensional domain in which the soft matrix is considered as empty (Carpinteri 1994a,b); for example, the dimension of the well-known Sierpinski carpet (Fig. 2), is $D = 1.89$.

Since $\sigma_{hN} n^N R_N^2 = \sigma_{hN} R_N^{2-D} R^D$ and $R/R_N = (n/\varphi)^{N/2}$, we derive:

$$\phi = \varphi^N = (R/R_N)^{D-2}. \tag{3}$$

Thus, from the equilibrium equation a scaling of the strength is predicted:

$$\sigma_C = \sigma_h \varphi^N + \sigma_s \left(1 - \varphi^N\right) = \sigma_h \,(R/R_N)^{D-2} + \sigma_s \left(1 - (R/R_N)^{D-2}\right). \tag{4}$$

Noting that $n > 1$ and $\varphi < 1$, we deduce $0 < D < 2$ and thus Eq. 2 predicts that "smaller is stronger" ($\sigma_h \gg \sigma_s$).

On the other hand, the *energy balance* implies $W \equiv A G_C = W_h + W_s = A_k G_{hk} + (A - N_k A_k)\, G_{sk} = N_N A_N G_{hN} + (A - N_N A_N)\, G_{sN},\ \forall k$, where W, W_h, W_s are, respectively the dissipated fracture energies in the bar, hard and soft phases, and G_C, $G_{hN} \equiv G_h$, $G_{sk} \equiv G_s$ ($\forall k$) are the fracture energies per unit area of the bar, hard and soft phases, respectively; usually $G_h \ll G_s$. Accordingly, the fracture energy must scale as:

$$G_C = G_h \varphi^N + G_s \left(1 - \varphi^N\right) = G_h \,(R/R_N)^{D-2} + G_s \left(1 - (R/R_N)^{D-2}\right). \tag{5}$$

And thus "larger is tougher". In the next section, toughening mechanisms will be introduced in the model.

On the other hand, the *compatibility equation* implies (bars in parallel): $K \equiv EA = K_h + K_s = N_k A_k E_{hk} + (A - N_k A_k)\, E_{sk} = N_N A_N E_{hN} + (A - N_N A_N)\, E_{sN},\ \forall k$, where K, K_h, K_s are respectively the "elastic" force of the bar, hard and soft phases and E, $E_{hN} \equiv E_h$, $E_{sN} \equiv E_s$ are the Young's moduli of the bar, hard and soft phases, respectively. Accordingly, the Young's modulus must scale as:

$$E = E_h \varphi^N + E_s \left(1 - \varphi^N\right) = E_h \,(R/R_N)^{D-2} + E_s \left(1 - (R/R_N)^{D-2}\right). \tag{6}$$

Since usually $E_h \gg E_s$, "smaller is stiffer".

Equations 4–6 show that at the smaller size-scales the inclusions are dominating, whereas at the larger size-scales the matrix dominates. These equations present the same self-consistent form: in fact, regarding the generic property X (σ_C, G_C or E) at the level $N-1$, $X_{N-1} = X_h\varphi + X_s(1-\varphi)$. Thus, at the level $N-2$: $X_{N-2} = X_{N-1}\varphi + X_s(1-\varphi) = X_h\varphi^2 + X_s\left(1-\varphi^2\right)$ and iterating $X \equiv X_0 = X_h\varphi^N + X_s\left(1-\varphi^N\right)$, as described by Eqs. 4–6. In addition, it is clear that the scaling laws predicted by Eqs. 4–6 are particularly reasonable, since they predict two asymptotic behaviours for macro- and nano size-scales. Note that for a three-dimensional architecture (i.e., particle inclusions and not longitudinal fibres) for which also the third dimension plays a role, in the stiffness of Eq. 6 the factor 2 must be replaced by 3, φ becomes the volume fraction rather than the cross-sectional fraction and D is deduced from Eq. 2 considering again the factor 3 instead of 2; this is true if we consider valid the rule of mixture of Eq. 6 also for a nonparallel architecture.

Then, the fracture toughness can be derived as $K_{IC} = \sqrt{G_C E}$, whereas the hardness $H \propto \sigma_C$ formally making the substitution $\sigma_C \to H$ in Eq. 4. Note that the important equality (3) would allow us to derive scaling laws from "rules of mixture" also in different systems and for different properties, e.g., the friction coefficient.

Finally, for quasi-fractal hierarchy, described by $n(R)$ and $\varphi(R)$ weakly varying with the size R, function $D(R)$ should be considered in Eqs. 4–6, as deducible from Eq. 2.

3 Toughening mechanisms: viscoelasticity, plasticity and crack deflection or bridging

Introducing a Young's modulus we have implicitly assumed linear elasticity. For a more realistic behaviour of the matrix, we should consider visco-elasticity, often observed in biotissues. If $\mu_v \equiv \left(E^0 - E^\infty\right)/E^\infty$, with E^0, E^∞ short- and long-time elastic moduli, respectively ($E^0 \geq E^\infty$, where the equality is valid for linear elasticity), the effective fracture energy becomes $G_s^+ = (1+\mu_v)\,G_s$. The parameter μ_v represents an enhancement factor for fracture energy dissipation due to the viscoelastic properties of the medium, e.g., for bone $\mu_v \approx 4$ or for shell $\mu_v \approx 1.5$ (see Ji and Gao 2004). Including plasticity, if μ_p represents the enhancement factor due to the plastic work during fracture $G_s^+ = (1+\mu)\,G_s$, where $\mu = \mu_v + \mu_p$. The factor μ_p can be estimated noting that the effect of plasticity on the crack propagation is described by a blunting of the crack tip due to dislocation emissions. If a is the "fracture quantum", a material/structural parameter, $\mu_p = \rho/(2a)$ (Pugno and Ruoff 2004), ρ being the tip radius.

According to the previous analysis and Fig. 1, the fracture surface is assumed to be planar. On the other hand, the inclusions could serve as hard structures to deflect the crack path or as crack bridging elements. In the latter case, the inclusions will be pulled-out after fracture, incrementing the dissipated energy in a fashion similar to the former mechanism (if fracture of the matrix is assumed similar to that of the interface; it is evident that this hypothesis can be easily removed). To model such effects, we simply assume the two-dimensional scheme reported in Fig. 3, which is a lateral view of the crack surface of Fig. 1. According to this scheme $G_s^{++}l = G_s^+(l+nh)$, where l is the nominal crack length, n is the number of inclusions along l and h is their height. Noting that $\varphi = nt/l$, with t thickness of the inclusions, and that $\lambda = h/t$ is their slenderness, the effective fracture energy becomes $G_s^{++} = (1+\lambda\varphi)\,G_s^+$. Thus, for this toughening mechanism, the fracture energy G_s^{++} can be even much larger ($\mu \approx \varphi \approx 1;\ \lambda \gg 1$) than the intrinsic fracture energy of the matrix G_s, if large values for λ are considered. This explains (Ji and Gao 2004) why the shape of

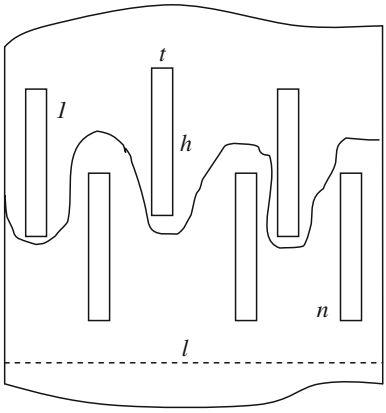

Fig. 3 The lateral view of the crack surface: toughening mechanics

mineral crystals is found to be very anisometric (platelets): the anisometry is larger for bone and dentin (platelets 3 nm thick and up to 100 nm long) as well as for enamel (15–20 nm thick, 1,000 nm long) than for nacre (i.e., see shells, 200–500 nm thick and 5–8 μm long). For details on the hierarchical bone structure, see Akkus et al. 2004. Thus, Eq. 5 in general has to be considered with the substitutions:

$$G_s \rightarrow (1+\mu)(1+\lambda\varphi)\, G_s \tag{7a}$$

$$G_h \rightarrow 0 \tag{7b}$$

since in this case no dissipation occurs in the hard phase.

Furthermore, a soft matrix activates shear mechanisms rather than longitudinal ones, according to the tension-shear chain model recently proposed (Ji and Gao 2004). Since in this case matrix does not carry tensile load, the substitution:

$$\sigma_s \rightarrow 0 \tag{8}$$

should be considered in Eq. 4. Considering a linear variation of the shear stress (but stress concentration factors could be included, Pugno and Carpinteri 2003) with a maximum value τ implies a maximum normal stress σ in the platelet equal to $\lambda\tau$ (Ji and Gao 2004). Thus, load transfer requires $\lambda\tau_s > \sigma_h$ where τ_s is the shear strength of the matrix; this shows that low values of τ_s are compensated in Nature by high slendernesses λ. Note that according to Ji and Gao (2004) an in-series tension/shear rather than an in-parallel tension architecture, as considered in Eq. 6, emerges. However, their asymptotic behaviours (for realistic sufficiently large size-scales R) are identical if in Eq. 6 the Young's modulus of the matrix is assumed to be negligible, i.e.

$$E_s \rightarrow 0 \tag{9}$$

4 Conclusions

The developed mathematical model, summarized in the numbered equations, allows us to preliminary design nano-bio-inspired hierarchical materials, by following a bottom-up procedure. The complexity of the problem has imposed a simplified treatment with associated

limitations; nevertheless, the model could be useful for preliminary designing micro- or nano-structured hierarchical materials.

References

Akkus O, Yeni YN, Wesserman N (2004) Fracture mechanics of cortical bone tissue: a hierarchical perspective. Crit Rev Biomed Eng 32:379–425
Brown JH, West GB (1999) Scaling in biology. Oxford University Press, Oxford
Carpinteri A (1994a) Fractal nature of material microstructure and size effects on apparent mechanical properties. Mech Mater 18:89–101
Carpinteri A (1994b) Scaling laws and renormalization groups for strength and toughness of disordered materials. Int J Solids Struct 31:291–302
Carpinteri A, Pugno N (2005) Are the scaling laws on strength of solids related to mechanics or to geometry? Nat Mater 4:421–423
Currey JD (1977) Mechanical-properties of mother of pearl in tension. Proc R Soc B 196:443–463
Currey JD (1984) The mechanical adaptations of bones. Princeton University Press, Princeton, NJ, pp. 24–37
Gao H (2006) Application of fracture mechanics concepts to hierarchical biomechanics of bone and bone-like materials. Int J Fract 138:101–137
Ji B, Gao H (2004) Mechanical properties of nanostructure of biological materials. J Mech Phys Solids 52:1963–1990
Lakes R (1993) Materials with structural hierarchy. Nature 361:511–515
Pugno N (2006) Mimicking nacre with super-nanotubes for producing optimized super-composites. Nanotechnology 17:5480–5484
Pugno N, Carpinteri A (2008) Design of micro/nano-bio-inspired hierarchical materials. Phil Mag Lett. doi:10.1080/09500830802089843
Pugno N, Carpinteri A (2003) Tubular adhesive joints under axial load. J Appl Mech 70:832–839
Pugno N, Ruoff R (2004) Quantized fracture mechanics. Philos Mag 84:2829–2845